

# Dual layered surface crystallization of 30BaO-15TiO<sub>2</sub>-55GeO<sub>2</sub> glass by stepwise heat treatment

著者	Masai Hirokazu, Fujiwara Takumi, Mori Hiroshi, Benino Yasuhiko, Komatsu Takayuki
journal or publication title	Journal of Applied Physics
volume	101
number	12
page range	123505
year	2007
URL	<a href="http://hdl.handle.net/10097/51962">http://hdl.handle.net/10097/51962</a>

doi: 10.1063/1.2743827

# Dual layered surface crystallization of 30BaO–15TiO<sub>2</sub>–55GeO<sub>2</sub> glass by stepwise heat treatment

Hirokazu Masai,<sup>a)</sup> Takumi Fujiwara, and Hiroshi Mori

Department of Applied Physics, Tohoku University, 6-6-05, Aoba, Sendai 980-8579, Japan

Yasuhiko Benino and Takayuki Komatsu

Department of Materials Science and Technology, Nagaoka University of Technology, 1603-1 Kamitomioka, Nagaoka 940-2188, Japan

(Received 12 February 2007; accepted 17 April 2007; published online 19 June 2007)

In the crystallization process of 30BaO–15TiO<sub>2</sub>–55GeO<sub>2</sub> (BTG55), we demonstrated by an x-ray diffraction analysis that a stepwise heat treatment enables a selective crystallization of fresnoite and benitoite, two crystalline phases obtained from the BTG55 mother glass and that these two phases form a dual surface layer. The result indicates that the stepwise heat treatment generates a compositional heterogeneity inside the glass matrix, which facilitates the nucleation of the fresnoite phase. The mechanism for the generation of the dual surface layer is discussed. Due to a marked difference in optical nonlinearity of the two phases, the selective crystallization may open the possibility of an optimized heat-treatment condition to achieve a large optical nonlinearity in crystallized glass. Also, two types of fresnoite, tetragonal and orthorhombic, were observed in the crystallized phase after a stepwise heat treatment of 690/720 °C. © 2007 American Institute of Physics. [DOI: 10.1063/1.2743827]

## I. INTRODUCTION

Crystallization from a supercooled liquid proceeds via nucleation and crystal growth by a decrease of free energy. If the chemical composition of a glass phase is nonstoichiometric with respect to the corresponding crystal, a surface crystallization tends to take place, because a nucleation at the surface of the glass occurs more easily than inside the matrix. Surface crystallization generally brings about a phase with oriented crystallites. If the orientation direction of a crystallized phase corresponds to the polar direction of the crystal, the obtained surface crystallized glasses are expected to exhibit a large macroscopic polarizability.<sup>1–7</sup> The crystallized glass possessing optical nonlinearity, therefore, can be a candidate for active optical materials if the orientation direction is controlled.<sup>1,4–7</sup>

Orientation in a surface crystallized glass is often explained with a geometric selection rule,<sup>8</sup> that is, a geometric texture development from the surface. According to the geometric selection rule, a crystal phase with the preferential direction grows faster than other crystalline phases, and consequently, dominates the orientation as well as the characteristic of the crystallized layer. However, neither the origin of the preferential direction nor the interaction between different crystallized phases has been clarified yet. For example, in the case of the transparent surface crystallized 30BaO–15TiO<sub>2</sub>–55GeO<sub>2</sub> (BTG55) glass, both fresnoite (Ba<sub>2</sub>TiGe<sub>2</sub>O<sub>8</sub>) and benitoite (BaTiGe<sub>3</sub>O<sub>9</sub>) crystallize from the same mother glass by a heat treatment.<sup>4–7</sup> Because the crystallization temperature of benitoite is lower than that of fresnoite, it is speculated that the crystallization of fresnoite from the surface is partially prevented by benitoite crystal-

lites and that some kind of interaction between two crystallized phases exists during the crystallization of fresnoite.

Recently, our group has reported a BTG55 crystallized glass with a highly oriented benitoite phase by a heat treatment at 690 °C for 3 h.<sup>7</sup> According to Robbins, BaTiGe<sub>3</sub>O<sub>9</sub> can be treated as isostructural with BaTiSi<sub>3</sub>O<sub>9</sub>,<sup>9,10</sup> and the barium ions in the orientated benitoite phase constitute a layered structure, which is similar to that of a *c*-oriented fresnoite phase. Figure 1 shows the crystal picture of benitoite from the point of directions (220), (202), (112), and (004). The dashed line shows the corresponding diffraction plane. It is noted that all the diffraction planes possess a layered structure consisting of barium ions. The crystallization behavior indicates the presence of an interaction between fresnoite and benitoite through the barium layered

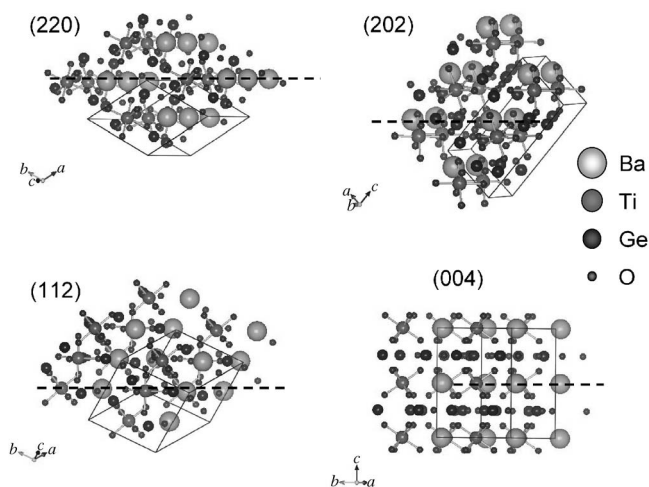


FIG. 1. The crystal picture of benitoite from the point of directions (220), (202), (112), and (004).

<sup>a)</sup> Author to whom correspondence should be addressed; FAX: +81-22-795-7963; electronic mail: masai@laser.apph.tohoku.ac.jp

structure. Here we define a system undergoing a surface crystallization involving two crystalline phases as a dual surface crystallization system. The BTG55 crystallized glass consisting of fresnoite ( $\text{Ba}_2\text{TiGe}_2\text{O}_8$ ) and benitoite ( $\text{BaTiGe}_3\text{O}_9$ ) is, therefore, a prototype system of a dual surface crystallization.

The purpose of this study is to examine the crystallization behavior of BTG55 glass in terms of the interaction between the fresnoite phase and benitoite phase. A stepwise heat treatment was performed at 690 and 720 °C to control the formation of the two crystallized phases. The amount as well as the orientation of the crystallized phases was evaluated by x-ray diffraction (XRD), and the mechanism of a dual layered crystallized structure by a stepwise heat treatment is discussed.

## II. EXPERIMENT

### A. Preparation and measurements of glass and crystallized glass

A BTG55 glass was prepared by a conventional melt-quenching method with starting materials  $\text{BaCO}_3$  (99.9%),  $\text{TiO}_2$  (99.9%), and  $\text{GeO}_2$  (99.95%). Batches were mixed and melted in a platinum crucible in an electric furnace at 1300 °C for 1 h. The glass melt was quenched on a steel plate held at 200 °C, and the obtained glass samples were annealed at the glass transition temperature,  $T_g$ , for 30 min. After annealing, the glass samples were cut into  $10 \times 10 \times \approx 1 \text{ mm}^3$  in size and mechanically polished to obtain a mirror surface using DOCTOR LAP ML-180 (Maruto).

The glass samples were heat treated on an alumina plate in a tubular furnace under an ambient atmosphere. After the heat treatment, the furnace was cooled down to room temperature at  $-4 \text{ K/min}$ . Since a crystalline phase was observed at both the front side (air side) and the back side (alumina side) of a heat-treated sample, the back side was mechanically polished to remove the crystalline phase completely and the front side was used for XRD measurements. Although the crystalline phase at the back side is similar to that of the front side, the front side was used to remove the possible effects of roughness and contamination at the interface.

The temperatures of glass transition  $T_g$ , crystallization onset  $T_x$ , and crystallization peak  $T_p$  were estimated by differential thermal analysis (DTA) operated at a heating rate of 10 K/min using TG8120 (Rigaku). The crystalline phases in glasses and crystallized glasses were examined by XRD with  $\text{Cu } K\alpha$  radiation. Second harmonic (SH) intensities of crystallized glass were evaluated by a Maker fringe technique in which Z-cut quartz (thickness of 0.6 mm) was used as a reference sample.<sup>4,6</sup> The crystallized side of the sample was irradiated with an yttrium aluminum garnet (YAG) laser at 1064 nm. The thickness of the crystallized layer was measured with cross-section observation of crystallized glass using a laser scanning microscope.

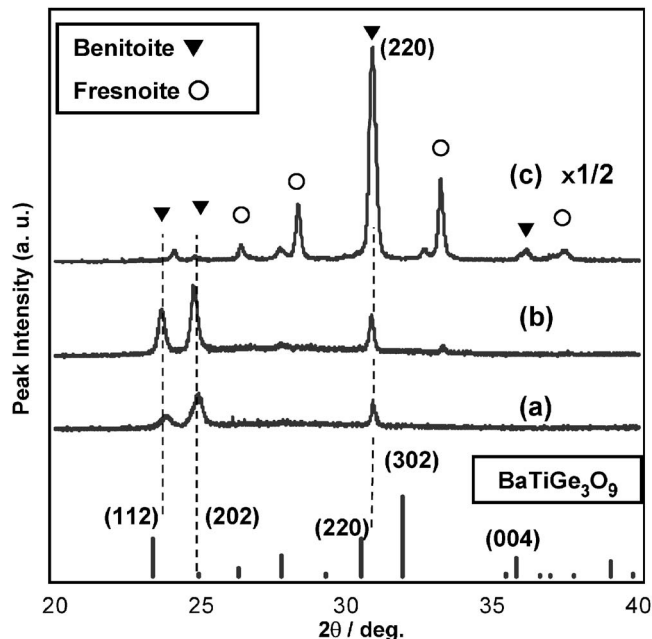


FIG. 2. XRD patterns of BTG55 crystallized glass heat treated at 690 °C for 3 (a), 6 (b), and 12 h (c) together with  $\text{BaTiGe}_3\text{O}_9$  (Ref. 11).

## III. RESULTS AND DISCUSSION

### A. BTG55 crystallized glass after a pre-heat-treatment at 690 °C

The obtained BTG55 and BTG55 crystallized glass obtained by a heat treatment at 690 °C were colorless and transparent.  $T_g$ ,  $T_x$ , and  $T_p$  of the BTG55 glass were determined as 667, 736, and 753 °C, respectively. Figure 2 shows XRD patterns of the BTG55 crystallized glass heat treated at 690 °C for 3, 6, and 12 h together with  $\text{BaTiGe}_3\text{O}_9$ .<sup>11</sup> Although the main diffraction peak of benitoite ( $\text{BaTiGe}_3\text{O}_9$ ) is (302) according Ref. 11, the observed main diffraction peak in the present study was not (302) but (220). No (302) diffraction peak was observed, indicating that surface crystallization has taken place. In the samples heat treated for 6 and 12 h, not only benitoite but also fresnoite ( $\text{Ba}_2\text{TiGe}_2\text{O}_8$ ) are observed, and the diffraction peak intensity of both benitoite and fresnoite increases with the increasing heat-treatment duration. The average size of crystallites in the crystallized phase is estimated using the Scherrer equation in which the crystallites are assumed to be spherical particles

$$D = \kappa\lambda/(\beta \cos \theta), \quad (1)$$

where  $D$  is the average size of crystallites,  $\kappa$  is the Scherrer coefficient,  $\lambda$  is the wavelength of x ray,  $\beta$  is the full width at half maximum of the peak, and  $\theta$  is the diffraction angle. Here, we use the Scherrer coefficient for spherical approximation as  $\kappa=0.9$ . Since the crystallites are assumed to be spherical, if the crystallites are anisotropic, the calculated diameter of anisotropic crystallites will be different for each plane. Table I shows the average diameters of benitoite crystallites in (112), (202), and (220) planes together with the average thicknesses of crystallized layers measured by observation with an optical microscope. The average crystallite size estimated from the (220) plane diffraction of the

TABLE I. The average diameters of benitoite crystallite in (112), (202), and (220) planes together with the average thickness of crystallized layer.

Pre-heat-treatment duration at 690 °C/h		3	6	12
Average diameter (nm)	(112)	20	31	54
	(202)	18	30	37
	(220)	55	55	33
Average thickness of crystallized layer ( $\mu\text{m}$ )		$2.0 \pm 0.3$	$2.3 \pm 0.5$	$3.5 \pm 0.4$

samples heat treated for 12 h is smaller than those of other crystallized glasses, indicating the presence of a size distribution of crystallites in the benitoite phase. Although there is a small difference in the crystallized layer thickness among three crystallized glasses, the XRD peak intensity of benitoite in the glass sample heat treated for 12 h is several-fold larger than in other crystallized glasses. These results indicate that the volume density of benitoite in the surface crystallized phase increases with increasing heat-treatment duration.

The chemical formula BTG55 can be broken down as the summation of stoichiometric crystals, *fresnoite* or *benitoite*, and the residual oxides. It can be written as either  $30\text{BaO}-15\text{TiO}_2-30\text{GeO}_2+25\text{GeO}_2$  or  $15\text{BaO}-15\text{TiO}_2-45\text{GeO}_2+15\text{BaO}+10\text{GeO}_2$ , where the stoichiometric composition of each corresponding crystalline phase is written in *italic*. Note that both *fresnoite* and *benitoite* can crystallize from the same mother glass, and the surplus oxides  $\text{GeO}_2$  and  $\text{BaO}$  are expected to be excluded from the crystalline region to the glass region during the nucleation. The surplus oxides affect the crystallization behavior, that is, the termination of a crystallized phase and the nucleation of other crystallized phases. Crystal growth from the surface generally terminates by a compositional mismatch near the interface between a crystalline region and a glass region. The present results show that the propagation range of the benitoite phase almost saturates after a heat treatment for 12 h at 690 °C. Since the barium ions must be excluded from the benitoite region to glass matrix during the crystallization, the forefront of the benitoite phase with uniform thickness becomes the barium rich region. In other words, the barium-rich region constitutes a pseudoplane consisting of barium ions. This plane, a layered structure consisting of barium ions, is thought to be favorable for the crystallization of the *c*-oriented *fresnoite*, which also has a layered structure consisting of barium ions.

In previous reports, only benitoite was observed in BTG55 crystallized glass after a heat treatment at 690 °C for 3 h, while *fresnoite* was observed only in the BTG55 crystallized glasses with a heat treatment for 3 h at temperatures above 700 °C.<sup>7</sup> The present result, however, shows that *fresnoite* can crystallize with a heat treatment at 690 °C for 6 and 12 h, indicating that barium ions excluded from the benitoite phase assist the crystallization of *fresnoite*. Note that the peak intensity ratio of (202) and (220) changes with increasing heat-treatment duration. After a heat treatment for 12 h, the main diffraction peak becomes (220), which has the diffraction plane containing the maximum number of barium ions<sup>7</sup> (see Fig. 1). It indicates that the (220) plane of benitoite

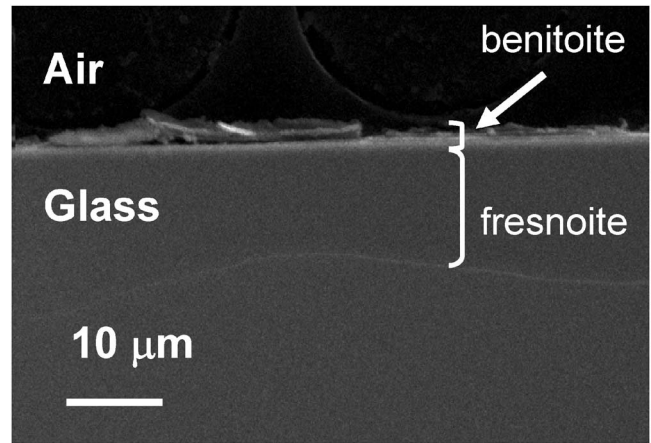


FIG. 3. SEM image of the cross section of the BTG55 crystallized glass heat treated at 690 °C for 6 h and 720 °C for 3 h.

takes a more stable state than other planes in the surface crystallized phase and that the replacement of benitoite crystallites takes place during the heat treatment.

### B. BTG55 crystallized glass after a post-heat-treatment at 720 °C

The BTG55 crystallized glass was obtained by a stepwise heat treatment; the stepwise heat treatment comprises of a pre-heat-treatment at 690 °C for 3 or 6 or 12 h followed by a post-heat-treatment at 720 °C for 3 h, in which the sample is cooled to room temperature between the pre- and post-heat-treatments. Figure 3 shows the scanning electron microscopy (SEM) image of the BTG55 crystallized glass with stepwise heat treatment at 690 °C for 6 h and at 720 °C for 3 h. As shown in Fig. 3, the crystallized layer consists of two layers, benitoite  $\text{BaTiGe}_3\text{O}_9$  and *fresnoite*  $\text{Ba}_2\text{TiGe}_2\text{O}_8$ . The thickness of an additional crystallized phase was estimated by an observation with an optical microscope as  $13 \pm 2 \mu\text{m}$  (3 h),  $12 \pm 2 \mu\text{m}$  (6 h), and  $9 \pm 2 \mu\text{m}$  (12 h), respectively. Figure 4 shows the XRD patterns of BTG55 crystallized glasses after stepwise heat treatment at 720 °C for 3 h together with those of orthorhombic *fresnoite* ( $\text{Ba}_2\text{TiGe}_2\text{O}_8$ , Ref. 12). Compared with the XRD patterns shown in Fig. 2, the several additional peaks that can be assigned to *fresnoite* are clearly observed. The *fresnoite* peak intensity of the crystallized glass pre-heat-treated for 12 h was weaker than that of the crystallized glass pre-heat-treated for 3 h. It indicates that the volume fraction of *fresnoite* near the surface depends on the pre-heat-treatment duration at 690 °C, namely, the volume density of the benitoite phase.

Note that an unknown peak ( $2\theta=33.7^\circ$ ,  $d=2.66 \text{ \AA}$ ) is observed near the orthorhombic *fresnoite* (002) diffraction peak in three spectra, while this peak was not observed in previous papers.<sup>4-7</sup> Such unknown peaks were also observed around (001), (003), and (004) diffraction peaks, and the differences of atomic distances calculated using the distance between the unknown peaks and the *c*-oriented orthorhombic *fresnoite* peaks are 0.08 Å (001), 0.04 Å (002), 0.28 Å (003), and 0.02 Å (004), respectively, indicating that these unknown peaks are correlated with the *c* orientation of orthorhombic *fresnoite*. Whereas the usual *fresnoite* family such



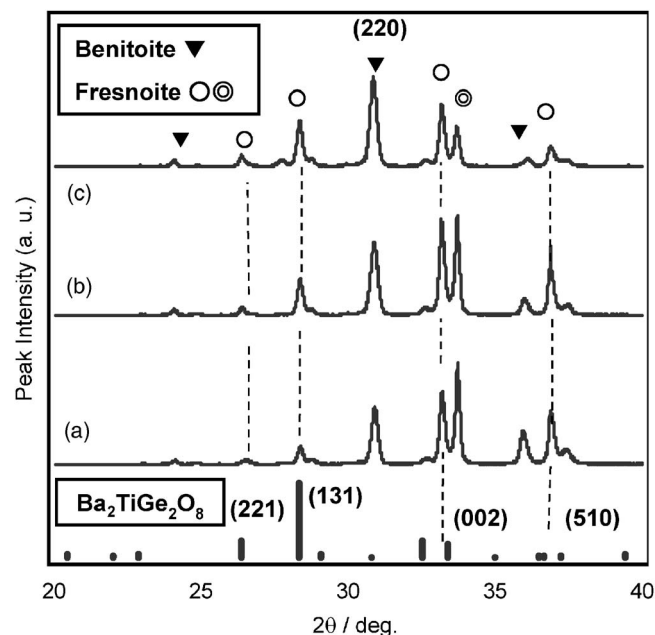


FIG. 4. XRD patterns of BTG55 crystallized glasses after stepwise heat treatment at 690 °C for 3 (a), 6 (b), and 12 h (c) and 720 °C for 3 h together with fresnoite ( $\text{Ba}_2\text{TiGe}_2\text{O}_8$ , Ref. 12).  $\odot$  mark is assigned to the diffraction of tetragonal  $\text{Ba}_2\text{TiGe}_2\text{O}_8$ .

as  $\text{Ba}_2\text{TiSi}_2\text{O}_8$  has a tetragonal crystal structure,<sup>13</sup>  $\text{Ba}_2\text{TiGe}_2\text{O}_8$ , one of the fresnoite families can take on two crystalline structures: orthorhombic<sup>12,14</sup> and tetragonal.<sup>15</sup> Although the atomic plane spacing in the (002) direction,  $d_{002}$ , is about 2.68 Å in both crystals, the plane spacing of the orthorhombic structure is slightly larger than that of the tetragonal structure. It has been reported that not only the crystalline structure but also the physical properties of crystallites in the crystallized phase are different from the corresponding bulk single crystals.<sup>16</sup> Here, we speculate that the difference of atomic distance was enhanced in the surface crystallized phase, and we assign the peak at  $2\theta=33.2^\circ$  ( $d_{002}=2.70$  Å) to the orthorhombic fresnoite (002) diffraction and another peak at  $2\theta=33.7^\circ$  ( $d_{002}=2.66$  Å) to the tetragonal (002) diffraction.

### C. Internal orientation of BTG55 crystallized glass after a post-heat-treatment at 720 °C

Figure 5(a) shows the XRD pattern of BTG55 crystallized glass after a pre-heat-treatment at 690 °C for 6 h (sample A), and Fig. 5(b) shows the XRD pattern of sample A with a post-heat-treatment at 720 °C for 3 h (sample B). Figures 5(c) and 5(d) show the XRD patterns of sample B after removal of the surface crystallized layer by polishing 5 (c) and 10  $\mu\text{m}$  (d), respectively. Since most of the benitoite peaks disappear and the peak intensity of the fresnoite phase increases after the surface polishing, the obtained XRD result also shows the existence of a dual crystallized phase consisting of benitoite and fresnoite in the BTG55 crystallized glass, as shown in Fig. 3. The effect of surface polishing upon the diffraction intensity is more pronounced for the tetragonal fresnoite (002) peak located at  $2\theta=33.7^\circ$ , compared with the orthorhombic fresnoite (002) diffraction peak

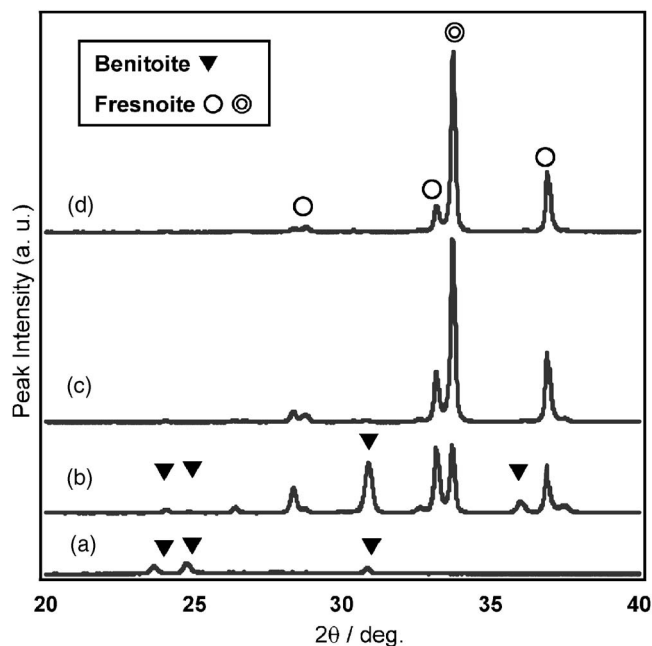


FIG. 5. XRD patterns of the BTG55 crystallized glass after pre-heat-treatment at 690 °C for 6 h (a), after post-heat-treatment at 720 °C for 3 h (b), and after surface polishing for 5 (c) and 10  $\mu\text{m}$  (d).  $\odot$  mark is assigned to the diffraction of tetragonal  $\text{Ba}_2\text{TiGe}_2\text{O}_8$ .

at  $2\theta=33.2^\circ$ . Moreover, this tetragonal fresnoite peak at  $2\theta=33.7^\circ$  survives after surface polishing of 10  $\mu\text{m}$ , that is, crystal growth occurred inside the glass matrix in the same manner as orthorhombic fresnoite. Thus, it can be concluded that two types of fresnoite, orthorhombic and tetragonal, crystallize in the surface crystallized phase layer.

Figure 6 shows the correlation between the peak intensity ratios of BTG55 crystallized glasses, which were pre-heat-treated at 690 °C for 6 h, and the surface removal thickness. The left axis shows the peak intensity ratio of the benitoite (220) and the orthorhombic fresnoite (002),  $b_{220}/f_{002}$ , and the right axis shows that of the tetragonal fresnoite (002) and the orthorhombic fresnoite (002),

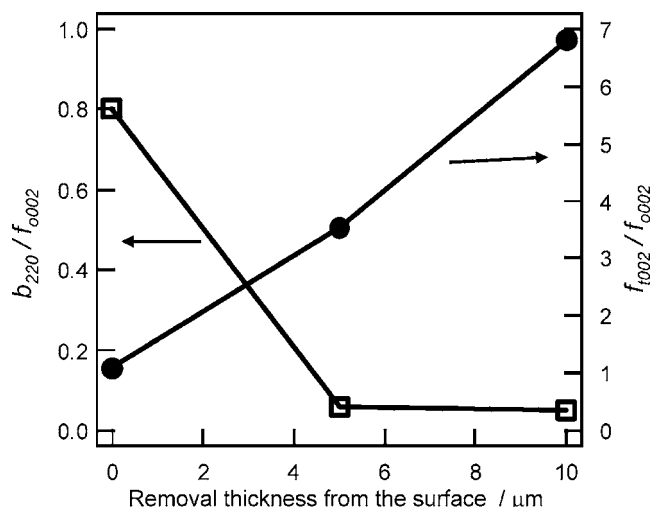


FIG. 6.  $b_{220}/f_{002}$  ratio and  $f_{1002}/f_{002}$  ratio as a function of removal thickness from the surface of BTG55 crystallized glass stepwise heat treated at 690 °C for 6 h, and then at 720 °C for 3 h.

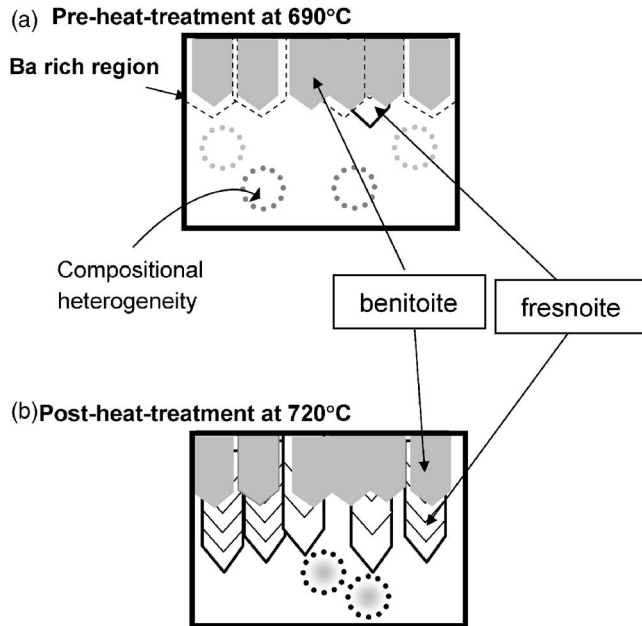


FIG. 7. The schematic image of stepwise crystallization in the present BTG55 glass.

$f_{i002}/f_{o002}$ . We first note that most of benitoite disappears after surface polishing of  $5\ \mu\text{m}$  and that a small amount of benitoite still exists after surface polishing beyond the average thickness of the crystallized phase. This result shows that the benitoite crystallites exist not only in the benitoite surface phase but also in other regions of the glass matrix. We also notice that the  $f_{i002}/f_{o002}$  ratio in Fig. 5 increases by the surface polishing, that is, the concentration of tetragonal fresnoite increases toward the depth direction of the sample.

#### D. Mechanism of crystallization in BTG55 glass with stepwise heat treatment

Here, we propose a mechanism that explains the increasing tetragonal fresnoite or the existence of benitoite in the crystallized glass based on the concept of compositional heterogeneity. The nanometer-scale heterogeneity of the glass, which can be crystal nuclei in the glass, was reported even in such a simple binary system as  $\text{SiO}_2\text{-GeO}_2$ .<sup>17</sup> If it is assumed that the structural rearrangement of atoms takes place after the pre-heat-treatment, the nucleation inside the matrix becomes easier than by a usual heat treatment, and as a result, benitoite or tetragonal fresnoite can be generated inside the matrix during the post-heat-treatment.

Figure 7 shows the schematic image of the stepwise crystallization in the present BTG55 glass. After pre-heat-treatment at  $690\ ^\circ\text{C}$ , the local area around benitoite becomes a barium-rich region, and the orthorhombic fresnoite crystallizes around benitoite crystallites. This is supported by the fact that tetragonal fresnoite is not observed after the pre-heat-treatment (see Fig. 2). Compositionally heterogeneous regions or small nuclei generate inside the glass matrix after pre-heat-treatment, and that region becomes a crystallite of tetragonal fresnoite or benitoite during the post-heat-treatment. Although this assumption may conflict with the present result of phase thickness in which pre-heat-treatment

of a sample with longer pre-heat-treatment has a smaller fresnoite thickness, the difference in propagation range of the fresnoite phase is explained by the diffusion of surplus ions, Ge and Ba. If the density of crystal nuclei at the surface is low, the surplus oxides are three dimensionally excluded from the crystalline region to the glass region, while the exclusion direction of other oxides becomes pseudo-one-dimensional when a surface crystallized phase with high nuclei density exists. It follows that the direction of exclusion matches the direction of propagation, and as a result, the excluded surplus ions prevent the propagation of the crystallized phase.

#### E. SH intensity of the orthorhombic and tetragonal $\text{Ba}_2\text{TiGe}_2\text{O}_8$ crystallized BTG55 glass

The orthorhombic-tetragonal phase transition has been studied in various kinds of single crystals in bulk form. For example, Kusainova *et al.* reported a correlation between the phase transition and second harmonic generation (SHG) property of an Aurivillius  $\text{Bi}_5\text{PbTi}_3\text{O}_{14}\text{Cl}$  crystal, and a reduction of the SHG signal was observed when the phase transition occurred from orthorhombic to tetragonal.<sup>18</sup> Although there is no previous report on the structure-SHG correlation in the  $\text{Ba}_2\text{TiGe}_2\text{O}_8$  crystal phase, a similar dependence is expected in the present  $\text{Ba}_2\text{TiGe}_2\text{O}_8$  crystallized glass, that is, the SHG of the orthorhombic crystallized BTG55 glass is stronger than that of the tetragonal crystallized BTG55 glass. The selective crystallization of orthorhombic  $\text{Ba}_2\text{TiGe}_2\text{O}_8$  crystallized glass is, therefore, favorable to the crystallized glass with a large second order optical nonlinearity.

To clarify the difference of the SH intensity originating from the  $\text{Ba}_2\text{TiGe}_2\text{O}_8$  phase of orthorhombic and tetragonal structures, the BTG55 crystallized glasses with different heat-treatment processes were prepared. One BTG55 crystallized glass (BTG55CG $\alpha$ ) was heat treated with the stepwise heat treatment, which has been mentioned above, and another crystallized glass (BTG55CG $\beta$ ) was heat treated with a continuous heating process, which comprises of a continuous heat treatment at  $690$  and  $720\ ^\circ\text{C}$  without the cooling process to room temperature. Figure 8(a) shows the XRD patterns of BTG55CG $\alpha$  and BTG55CG $\beta$ . In BTG55CG $\alpha$ , the tetragonal  $\text{Ba}_2\text{TiGe}_2\text{O}_8$  is clearly observed, whereas only a small amount of tetragonal  $\text{Ba}_2\text{TiGe}_2\text{O}_8$  is observed in BTG55CG $\beta$ . The thickness of the surface layer in BTG55CG $\beta$  is  $12\pm 2\ \mu\text{m}$ , which is comparable to that of BTG55CG $\alpha$ . Figure 8(b) shows Maker fringe patterns of BTG55CG $\alpha$  and BTG55CG $\beta$ . It shows that the SH intensity of BTG55CG $\beta$  is larger than that of BTG55CG $\alpha$ , which has been heat treated with a cooling process. Since the SH intensity is normalized by the incident laser power and since the thickness of the surface crystallized layer of both samples is about the same, the difference of the obtained SH intensity is thought to be caused by the structure of crystallized phase. It follows that the BTG55 crystallized glass with orthorhombic fresnoite shows larger optical nonlinearity than that with tetragonal fresnoite, and that this result is consistent with that of Kusainova *et al.* Therefore, the present study clearly indi-

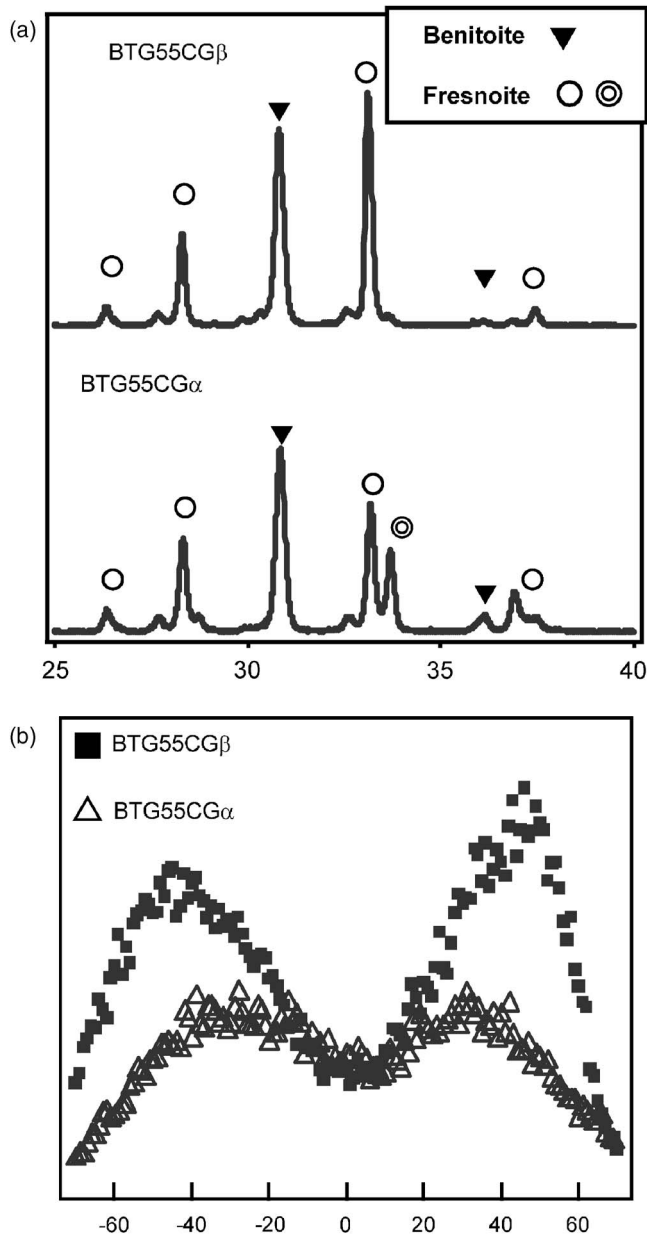


FIG. 8. (A) XRD patterns of BTG55CG $\alpha$  and BTG55CG $\beta$  heat treated at 690 °C for 12 h and at 720 °C for 3 h. (B) Maker fringe patterns of BTG55CG $\alpha$  and BTG55CG $\beta$  heat treated at 690 °C for 12 h and at 720 °C for 3 h. BTG55CG $\alpha$  was heat treated with a stepwise heat-treatment cooling to room temperature, whereas BTG55CG $\beta$  was heat treated with a continuous heating process, which comprises of a continuous heat treatment at 690 and 720 °C without the cooling process to room temperature.

cates that the crystallized phase that dominates the corresponding optical nonlinearity of the crystallized glass can be controllable by heat-treatment conditions.

#### IV. CONCLUSION

The effect of a stepwise heat-treatment process upon the crystallization behavior of BTG55 glass was investigated using XRD. It is suggested that a barium-rich region, which is favorable for the crystallization of orthorhombic fresnoite, is formed around benitoite crystallites. After the stepwise heat treatment, both orthorhombic and tetragonal fresnoite were observed and the tetragonal fresnoite preferentially propagated into the glass matrix. Crystallization of a tetragonal fresnoite indicates that the compositionally heterogeneous regions or the crystal nuclei formed inside the glass matrix by the stepwise heat treatment assist the crystallization of fresnoite. The present results indicate that the heat-treatment procedure affects the crystallized phase and the corresponding optical nonlinearity.

#### ACKNOWLEDGMENTS

This work was partially supported by the Grant-in-Aid for Scientific Research from the Ministry of Education, Science, Sport and Culture, Japan, the SCOPE (Strategic Information and Communications R&D Promotion Program) project by the Ministry of Public Management, Home Affairs, Posts and Telecommunications, Japan, and the research collaboration with Asahi Glass Co. LTD.

- <sup>1</sup>Y. Takahashi, Y. Benino, T. Fujiwara, and T. Komatsu, *Appl. Phys. Lett.* **82**, 223 (2002).
- <sup>2</sup>Y. Li, W. V. Youdelis, B. S. Chao, and H. Yamauchi, *J. Am. Ceram. Soc.* **76**, 2985 (1993).
- <sup>3</sup>S. Senz, A. Graff, W. Blum, D. Hesse, and H.-P. Abicht, *J. Am. Ceram. Soc.* **81**, 1317 (1998).
- <sup>4</sup>Y. Takahashi, Y. Benino, T. Fujiwara, and T. Komatsu, *J. Non-Cryst. Solids* **316**, 320 (2003).
- <sup>5</sup>Y. Takahashi, Y. Benino, T. Fujiwara, and T. Komatsu, *J. Appl. Phys.* **95**, 3503 (2004).
- <sup>6</sup>H. Masai, T. Fujiwara, Y. Benino, and T. Komatsu, *J. Appl. Phys.* **100**, 023526 (2006).
- <sup>7</sup>H. Masai, T. Fujiwara, Y. Benino, T. Komatsu, and H. Mori, *J. Appl. Phys.* **101**, 033530 (2007).
- <sup>8</sup>A. B. R-Navarro, *Thin Solid Films* **389**, 288 (2001).
- <sup>9</sup>C. R. Robbins, *J. Am. Ceram. Soc.* **43**, 610 (1960).
- <sup>10</sup>C. R. Robbins and E. M. Levin, *J. Res. Natl. Bur. Stand., Sect. A* **65**, 127 (1961).
- <sup>11</sup>JCPDS Card No. 00-013-0475 (unpublished).
- <sup>12</sup>JCPDS Card No. 01-077-0389 (unpublished).
- <sup>13</sup>P. B. Moore and J. Louisnathan, *Science* **156**, 3780 (1967).
- <sup>14</sup>K. Iijima, F. Marumo, M. Kimura, and T. Kawamura, *Nippon Kagaku Kaishi* **10**, 1557 (1981) (in Japanese).
- <sup>15</sup>JCPDS Card Nos. 00-020-0151 and 00-035-0213 (unpublished).
- <sup>16</sup>A. Halliyal, A. Safari, A. S. Bhalla, R. E. Newnham, and L. E. Cross, *J. Am. Ceram. Soc.* **67**, 331 (1984).
- <sup>17</sup>H. Hosono, K. Kawamura, H. Kawazoe, and J. Nishii, *J. Appl. Phys.* **80**, 3115 (1996).
- <sup>18</sup>A. K. Kusainova, S. Y. Stefanovich, J. T. S. Irvine, and P. Lightfoot, *J. Mater. Chem.* **12**, 3413 (2002).